BMC Nephrology

RESEARCH

Open Access

Single-cell RNA sequencing analysis of peripheral blood mononuclear cells in PD-1-induced renal toxicity in patients with lung cancer

Shusu Liu[1†], Peiyu Lu[1†], Bixia Yang[1], Yan Yang[1], Hua Zhou[1] and Min Yang[1*]

Abstract

Background Although the patient survival rate for many malignancies has been improved with immune checkpoint inhibitors (ICIs), some patients experience various immune-related adverse events (irAEs). IrAEs impact several organ systems, including the kidney. With anti-programmed cell death protein 1 (PD-1) therapy (pembrolizumab), kidney-related adverse events occur relatively rarely compared with other irAEs. However, the occurrence of AKI usually leads to anti-PD-1 therapy interruption or discontinuation. Therefore, there is an urgent need to clarify the mechanisms of renal irAEs (R-irAEs) to facilitate early management. This study aimed to analyse the characteristics of peripheral blood mononuclear cells (PBMCs) in R-irAEs.

Methods PBMCs were collected from three patients who developed R-irAEs after anti-PD-1 therapy and three patients who did not. The PBMCs were subjected to scRNA-seq to identify cell clusters and differentially expressed genes (DEGs). Kyoto Encyclopedia of Genes and Genomes (KEGG) and gene ontology (GO) enrichment analyses were performed to investigate the most active biological processes in immune cells.

Results Fifteen cell clusters were identified across the two groups. *FOS*, *RPS26*, and *JUN* were the top three upregulated genes in $CD4^+$ T cells. The DEGs in $CD4^+$ T cells were enriched in Th17 differentiation, Th1 and Th2 cell differentiation, NF-kappa B, Nod-like receptor, TNF, IL-17, apoptosis, and NK cell-mediated cytotoxicity signaling pathways. *RPS26*, *TRBV25-1*, and *JUN* were the top three upregulated genes in $CD8^+$ T cells. The DEGs in $CD8^+$ T cells were enriched in Th17 cell differentiation, antigen processing and presentation, natural killer cell-mediated cytotoxicity, the intestinal immune network for IgA production, the T-cell receptor signalling pathway, Th1 and Th2 cell differentiation, the phagosome, and cell adhesion molecules.

Conclusions In conclusion, R-irAEs are associated with immune cell dysfunction. DEGs and their enriched pathways identified in $CD4^+$ T cells and $CD8^+$ T cells play important roles in the development of renal irAEs related to anti-PD-1 therapy. These findings offer fresh perspectives on the pathogenesis of renal damage caused by anti-PD-1 therapy.

†Shusu Liu and Peiyu Lu contributed equally to this work.

*Correspondence:
Min Yang
yangmin1516@suda.edu.cn

Full list of author information is available at the end of the article

Keywords Acute kidney injury, Immune-related adverse events, Immune checkpoint inhibitors, Single-cell RNA-seq, Immune cells

Introduction

The emergence and clinical use of immune checkpoint inhibitors (ICIs) have changed the current status of cancer treatment [1]. Cytotoxic T-lymphocyte-associated protein 4 (CTLA-4), programmed death-ligand 1 (PD-L1), and programmed cell death protein 1 (PD-1) inhibitors are classic ICIs that are widely used clinically [2]. Over the last several years, several ICIs have been approved by the US Food and Drug Administration (FDA) for the treatment of small- cell and non-small cell lung cancers, urothelial carcinoma, renal cell carcinoma, classical Hodgkin's lymphoma, melanoma, and other cancers [3].

$CD4^+$ T cells, $CD8^+$ T cells, regulatory T (Treg) cells, natural killer (NK) cells and B cells all express PD-1 [4]. While binding to either of its ligands, namely, PD-L1 (CD274 and B7-H1) and PD-L2 (CD273 and B7-DC), PD-1 maintains peripheral tolerance by suppressing T-cell proliferation, activation, and effector functions [5]. The interaction between PD-1 and PD-L1 suppresses the immune response, leading to tumour escape and proliferation [6]. ICIs inhibit the negative regulation of T cells and exert anticancer effects.

ICIs improve cancer prognosis but are also induce a series of complications called immune-related adverse events (irAEs) [7]. IrAEs can be defined as immune-mediated host organ dysfunction occurring secondary to immune therapy-related abnormal immune system activity [8]. Common sites of irAEs include the skin, endocrine glands, lungs, liver, and gastrointestinal tract [9–13], but other organ systems, such as the cardiovascular and renal systems, can also be affected [14, 15]. Although most irAEs resolve with immunosuppressant use (e.g., corticosteroids) or are self-limiting, they may be associated with irreversible organ damage or death in rare cases [16, 17].

Renal irAEs (R-irAEs) are relatively rare, and other organs are more likely to be affected [1;18]. Most cases of R-irAEs are asymptomatic; notably, sterile pyuria and increased serum creatinine (Scr) are the only clinical signs of R-irAEs [18]. ICI-associated acute kidney injury (AKI) is the most common kidney irAE reported in the Adverse Events Reporting System of the US FDA [19]. Renal biopsy confirms acute interstitial nephritis (AIN) as the most common presentation of ICI-associated AKI [20]. Other histological lesions, including thrombotic microangiopathy, minimal change disease (MCD), and membranous nephropathy (MN), have also been reported [21, 22]. The exact mechanisms of renal damage related to ICI treatment remain unknown.

Single-cell RNA sequencing (scRNA-seq) is a novel technology that is widely used for discovering heterogeneity in the response to cancer immunotherapy at the single-cell level. ScRNA-seq may provide new insights into the immunologic landscape of ICI-mediated nephrotoxicity. In this study, we systematically evaluated the immune characteristics associated with PD-1-induced nephrotoxicity in the peripheral blood of lung cancer patients. Our data provide a rich resource for exploring the pathogenesis of R-irAEs related to anti-PD-1 therapy.

Materials and methods

Patients

In this study, we included three lung cancer patients with PD-1 inhibitor-induced R-irAEs and three lung cancer patients treated with anti-PD-1 therapy (pembrolizumab) but did not develop R-irAEs (the ctrl group). Details of the six patients are presented in Table S1. For multifactorial matching (comorbidities, potential nephrotoxic drugs), the patients selected were male. All patients were recruited from the Third Affiliated Hospital of Soochow University.

Patients were diagnosed with ICI-induced AKI according to the Common Terminology Criteria for Adverse Events v.4.0 definition [23]: a serum creatine (sCr) increase > 0.3 mg/dl or sCr > 1.5× baseline. The last stable serum creatinine value before PD-1 therapy was defined as the baseline creatinine value. Owing to ICI-induced AKI, pembrolizumab therapy was discontinued. Renal recovery was defined as a nadir sCr ≤ 1.5× baseline within 90 days following ICI-induced AKI.

The ethics committee of the Third Affiliated Hospital of Soochow University (Grant No. 2022[039]) approved this study. The study protocol adhered to the Declaration of Helsinki. All patients provided signed informed consent. Blood samples were collected after informed consent was obtained. Medical history information was obtained by accessing the electronic medical records system.

PBMC isolation

Patient blood was collected on the first day of each hospitalization. Blood samples from the participants were collected in an ethylenediaminetetraacetic acid (EDTA) anticoagulant tube for subsequent processing and analysis. Then, the PBMCs were separated on the day of blood collection, and Ficoll–Paque density gradient centrifugation was used to isolate the PBMCs. Cell viability was assessed by microscopic examination using Taipan blue staining. Finally, samples with more than 85% viable cells

were used to prepare single-cell RNA-seq (scRNA-seq) libraries.

Processing and quality control of scRNA-seq data

ScRNA-seq libraries were generated using the Chromium Single-Cell 3' Library and Gel Bead Kit v2 (10×Genomics, Pleasanton, CA) according to the manufacturer's instructions. The libraries were subsequently sequenced on the Illumina NovaSeq 6000 system. Cell Ranger (version 5.0.0) from 10×Genomics was applied to process the raw gene expression matrices from each sample's sequencing data. The R package Seurat (version 4.0.0) was used to process the unique molecular identifier (UMI) counting matrix, which was then used for quality control, normalization, dimensional reduction, batch effect removal, clustering, and visualization. DecontX, a novel Bayesian approach, was applied to eliminate the contamination in individual cells. To exclude low-quality captures and eliminate the possibility of multiple captures, cells were filtered out according to the following criteria: (1) gene numbers less than 400, (2) gene numbers greater than 6000, (3) UMI greater than 50,000, (4) percentage of mitochondrial RNA UMIs greater than 10%, (5) percentage of ribosome RNA UMIs greater than 40%, and (6) percentage of contamination in each cell greater than 20%. The "Normalize Data" function in Seurat was subsequently used to normalize and assess the library size. Elimination of batch effects between individuals was achieved by identifying anchors between individuals and passing them to the "IntegrateData" function.

Clustering analysis and visualization

The "FindClusters" function in Seurat was used to perform graph-based clustering on the basis of the gene expression profile of cluster cells. Data visualization was performed with the uniform manifold approximation and projection (UMAP) algorithm, and marker genes for each cluster were identified via the "FindAllMarkers" function in Seurat. We used CellTypist to annotate cells via built-in scRNA-seq models (with a focus on immune subpopulations) [24]. Three models were used: COVID19_Immune_Landscape, COVID19_Human-Challenge, Healthy_COVID19_PBMC. After the main cell types were labelled, we performed clustering analysis of the $CD4^+$ T cells. Cell populations with both CD4 and CD8A or S100A8 and CD68 expression were regarded as doublets and discarded. In addition, cells with a relatively high percentage of mitochondria were annotated as high.mt. The cell populations were indicated as follows: CCR6, KLRB1 and RORA expression indicated Th17 cells; ANXA1 and GATA3 expression indicated Th2 cells; FOXP3 and CTLA4 expression indicated Treg cells; GNLY, NKG7 and GZMB expression indicated cytotoxic $CD4^+$ T cells (CTL-CD4); And high AQP3, ITGA4, PDCD1 and LIMS1 expression indicated LIMS1-CD4 T cells, similar to the T09 cluster (Identifying CNS-colonizing T cells as potential therapeutic targets to prevent progression of multiple sclerosis - ScienceDirect); these cells may also be similar to Treg cells, which express the checkpoint genes PDCD1 and TIGIT.

Differentially expressed genes (DEGs) analysis

DEGs across different clusters were selected via the "FindMarkers" function in Seurat. The adjusted *P* values of the Wilcoxon rank sum test <0.05 and $|\log2FC| > 0.2$ indicated significant differences.

Functional enrichment analysis of DEGs

Gene Ontology (GO) and Kyoto Encyclopedia of Genes and Genomes (KEGG) analyses were performed for functional annotation analysis of the DEGs. Pathway enrichment analysis was performed with the R "phyper" function upon hypergeometric distribution, and enrichment analysis of GO categories was performed via R clusterProfiler (v3.14.3). False detection rates of <0.05 and *P* values of <0.05 were considered to indicate significant enrichment in GO terms and KEGG pathways. DEGs ≥ 5 were saved for GO classification or pathway analyses.

Results

Single-cell profiling of PBMCs

To explore the immune profile of R-irAEs related to PD-1 treatment, three patients with R-irAEs and three patients without R-irAEs were recruited for our study. PBMCs obtained from these patients were subjected to scRNA-seq (Fig. 1A). We filtered out low-quality cells according to the previously mentioned criteria (Figure S1). After quality control, a total of 35,088 cells were included and 15 clusters were identified (Fig. 1B). The dominant cell types were B cells, CD14-mono cells, CD16-mono cells, $CD4^+$ T cells, $CD8^+$ T effector memory cells (CD8-Tem cells), $CD8^+$ T cells, naïve $CD8^+$ T cells (CD8-Tn cells), cycling cells, dendritic cells (DCs), gdT cells, megakaryocytes, neutrophils, NK cells, plasmacytoid dendritic cells (pDCs), and plasma B cells. These clusters were classified into R-irAE and ctrl groups (Fig. 1C). The UMAP plot of the canonical markers is shown in Fig. 2A. The cell types and their markers were as follows: $CD4^+$ T cells: CD3D and CD4; $CD8^+$ T cells: CD8A; CD8-Tn cells: LEF1; CD8-Tem cells: GZMK; NK cells: NCAM1; gdT cells: TRGV9; B cells: CD79A; plasma B cells: MZB1; pDCs: CLEC4C; DCs: CD1C; neutrophils: G0S2; CD14-momo: CD14; CD16-mono: FCGR3A; Megakaryocytes: GP9; and cycling cells: MKI67 Fig. 2.

Changes in cellular proportion

Fig. 3A shows the cell distribution in the two groups. We compared the differences in the proportions of the 15 cell

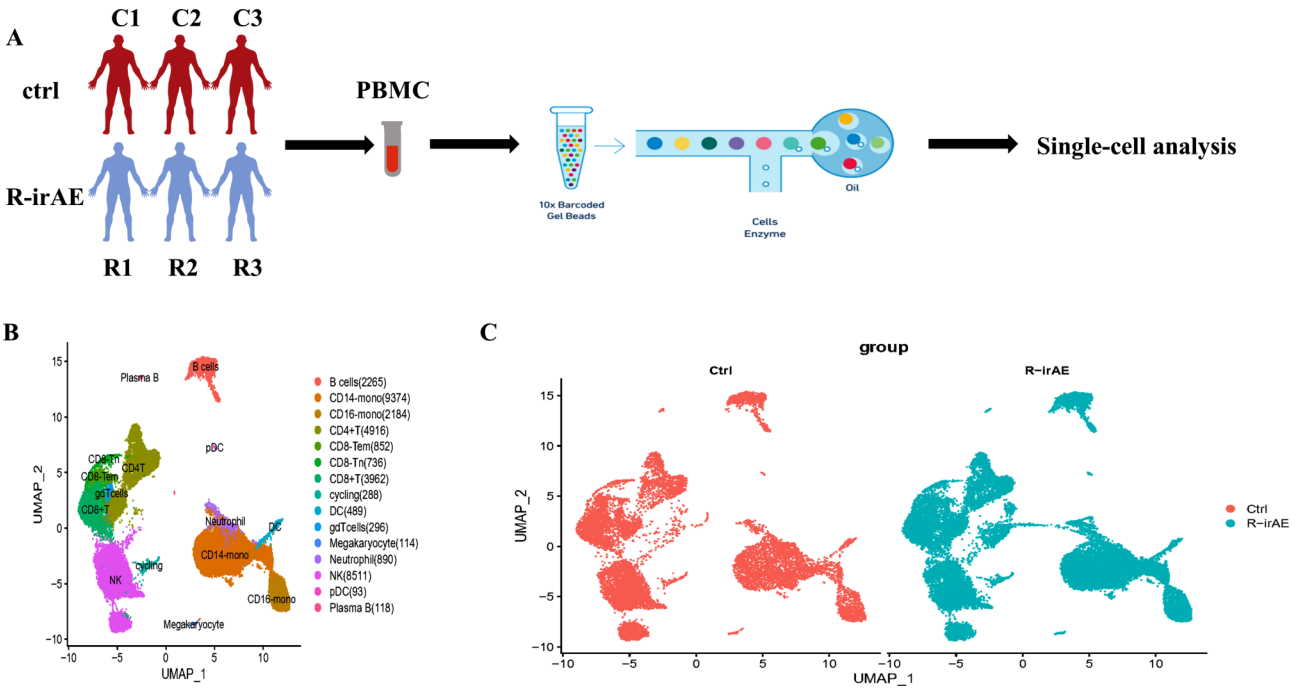

Fig. 1 Study design and landscape. (**A**) Study design. (**B**) All 15 clusters were identified and are shown in the UMAP plot. Each colour represents a different cluster, and each dot represents a single cell. (**C**) Cell distribution in the ctrl and R-irAE groups shown in the UMAP plot

types between the two groups and noted that there were no significant differences (Fig. 3B). The distributions of various cell types in each sample are shown in Fig. 3C.

DEGs observed in patients who experienced R-irAEs

We used differential expression analysis across groups to analyse variations in gene expression profiles within each cell type. DEGs were identified as described in the Materials and methods section ($|\log2FC| > 0.2$ and adjusted P value < 0.05). We identified many DEGs in each cell type (Fig. 4A), with the greatest number of DEGs noted in neutrophils.

Anti-PD-1 therapy may induce kidney injury by activating T cells [25]. A previous report revealed that the pathological manifestation of AKI was AIN in 12 patients due to nivolumab, ipilimumab, or combination therapy; these 12 patients harboured a total of 13 malignant tumours, which were predominantly infiltrated with lymphocytes along with plasma cells and eosinophils [26]. In addition, immunohistochemistry revealed $CD3^+$ T lymphocyte infiltrates in the interstitium of the kidney biopsy samples from patients with ICI-induced AKI, and these infiltrates predominantly contained $CD4^+$ T cells. In a previously published case report, a patient with metastatic malignant melanoma received a combination of anti-PD-1-antibody and anti-CTLA-4 antibody therapy; this patient developed acute tubulointerstitial nephritis, with $CD4^+$ T-cell and $CD8^+$ T-cell infiltration confirmed by renal biopsy and flow cytometry analyses [25]. Consequently, we concentrated on $CD8^+$ T and $CD4^+$ T cells in subsequent studies. To identify the transcriptomic differences between the two groups, functional enrichment analysis of the DEGs was performed.

Characteristics and biological functions of CD4+ T cells

We next explored DEGs in $CD4^+$ T cells between the two groups. In total, 303 DEGs (158 downregulated genes and 145 upregulated genes) were identified in $CD4^+$ T cells between the R-irAE and ctrl groups (Fig. 4A). The top three enriched upregulated genes were *FOS*, *RPS26*, and *JUN* (Fig. 5A). *FOS* and *JUN* are involved in the proliferation, development, and activation of lymphocytes, which contribute to immune system functions [27]. *RPS26* encodes a ribosomal protein involved in growth and development [28].

The enrichment analysis suggested that the DEGs of the $CD4^+$ T cells were enriched in gene sets related to Th17 cell differentiation, Th1 and Th2 cell differentiation, the NF-kappa B signalling pathway, the Nod-like receptor signalling pathway, the TNF signalling pathway, IL-17 signalling pathway, apoptosis, and the NK cell-mediated cytotoxicity signalling pathway (Fig. 5B). Various biological processes, such as T cell activation and cell death, are controlled by these DEGs, as shown in Fig. 5C.

For further analysis, $CD4^+$ T cells were reclustered and annotated. scRNA-seq analysis detected 4480 cells in the two groups, and accordingly, six subsets were defined, namely, CD4-CTL cells, CD4-Tn cells,

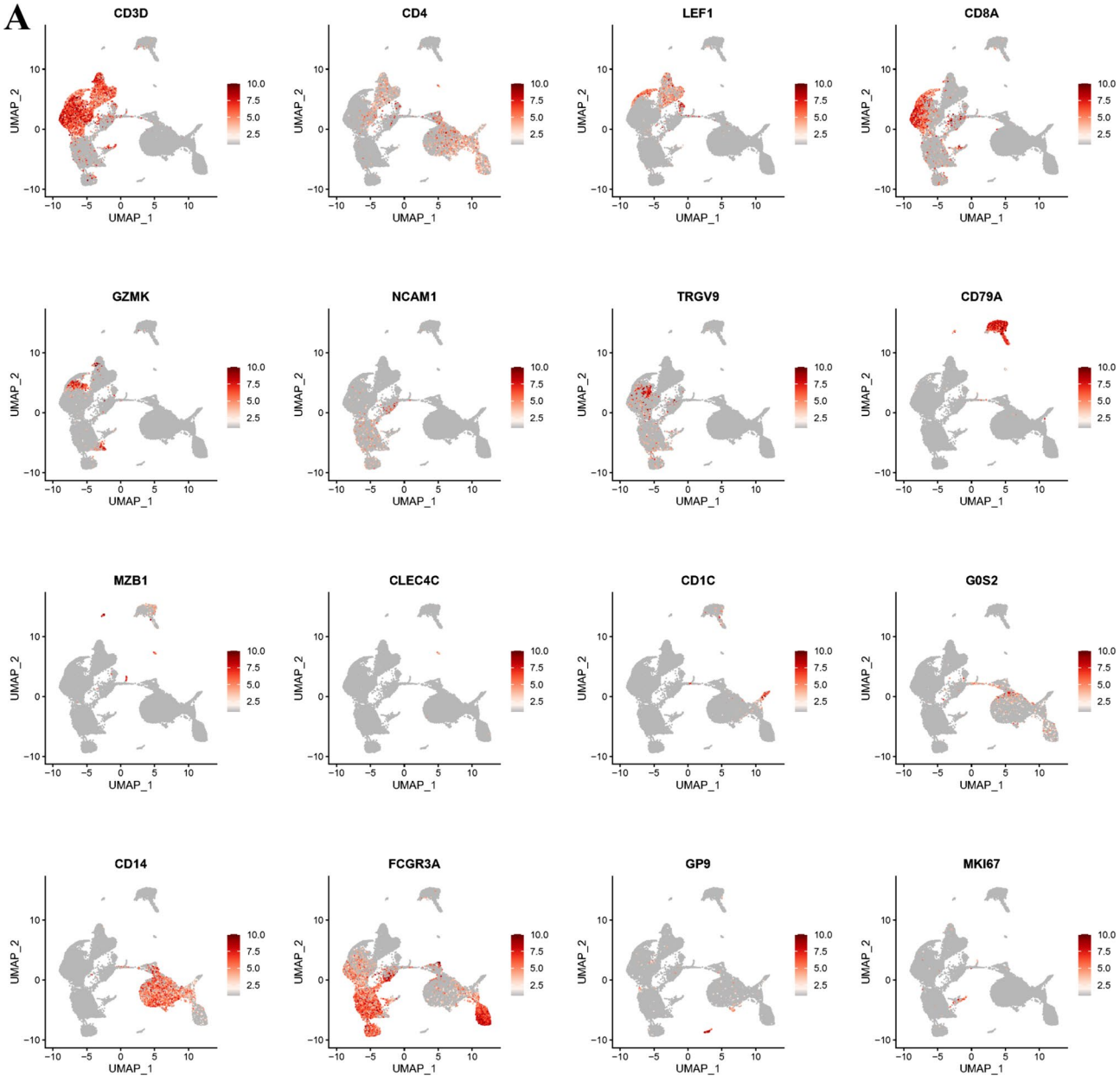

Fig. 2 Distribution and expression of canonical markers in different clusters. (**A**) Cell markers and cell types—$CD4^+$ T cells: CD3D and CD4; $CD8^+$ T cells: CD8A; CD8-Tn cells: LEF1; CD8-Tem cells: GZMK; NK cells: NCAM1; gdT cells: TRGV9; B cells: CD79A; plasma B cells: MZB1; pDCs: CLEC4C; DCs: CD1C; neutrophils: G0S2; CD14-momo: CD14; CD16-mono: FCGR3A; Megakaryocytes: GP9; cycling cells: MKI67

LIMS1-CD4 cells, Th2 cells, Th17 cells, and Treg cells (Fig. 6A, B). Figure 6C displays the distribution of these cells in the R-irAE and ctrl groups. The percentage changes in the six cell types were subsequently compared between the R-irAE group and the ctrl group (Fig. 6D).

The 155 downregulated genes and 68 upregulated genes in CD4-CTL cells between the R-irAE and ctrl groups are shown in Fig. 7A. Notably, 174 downregulated genes and 216 upregulated genes were found in CD4-Tn cells; 8 downregulated genes and 38 upregulated genes were discovered in LIMS1-CD4 T cells; 38 downregulated genes and 45 upregulated genes were found in Th2 cells; 2 downregulated genes and 7 upregulated genes were found in Th17 cells; and 37 downregulated genes and 28 upregulated genes were found in Treg cells.

RPS26, *TRBV20-1*, and *HLA-DRA* were the top three upregulated genes in CD4-CTL cells (Fig. 8A). *HLA-DRA* is expressed on the surface of various antigen presenting cells and plays a central role in the immune system and response by presenting peptides derived

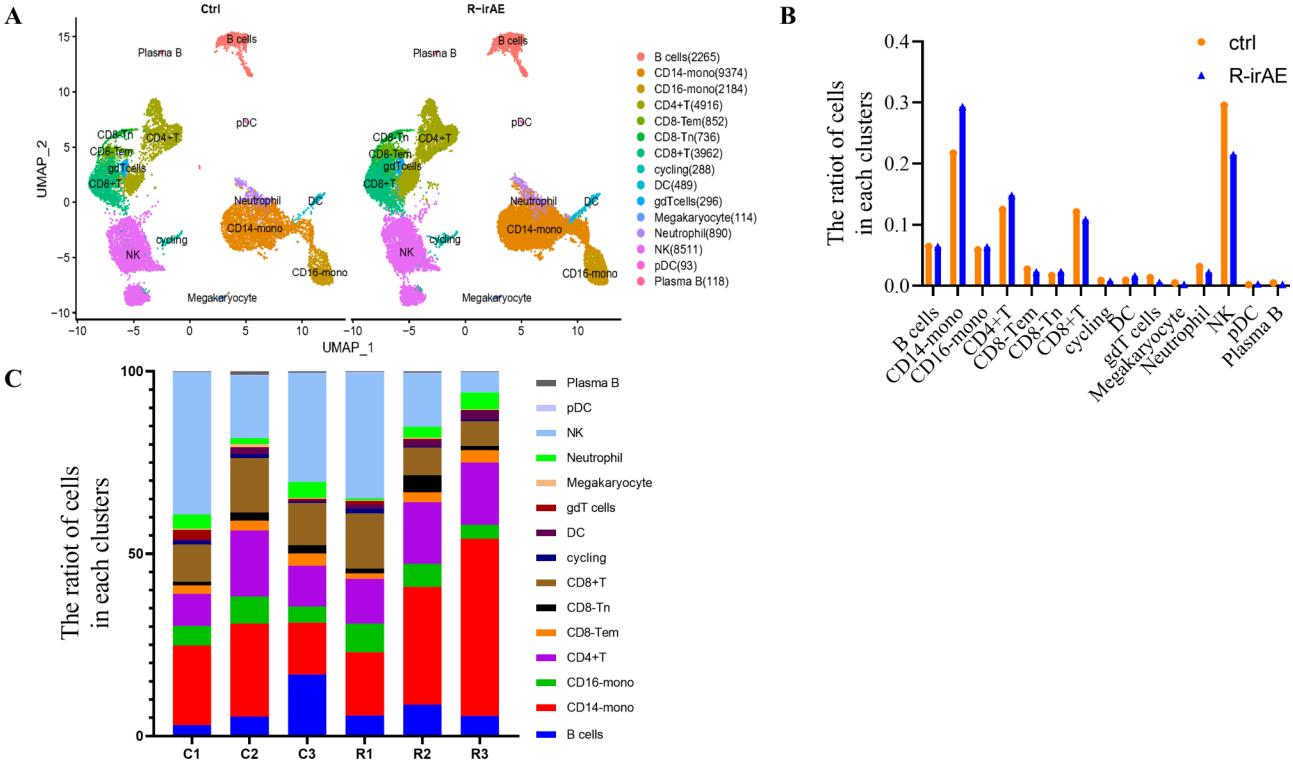

Fig. 3 Differences in cell composition across disease conditions. (**A**) Cell types from the ctrl and R-irAE groups with the UMAP plot. The plot is coloured according to the cell type, and each dot corresponds to a single cell. (**B**) Column graphs showing the relative percentage of each cell type in the ctrl and R-irAE groups. There was no significant difference between the two groups. (**C**) Stacked bar graphs showing the cell type distributions in each sample

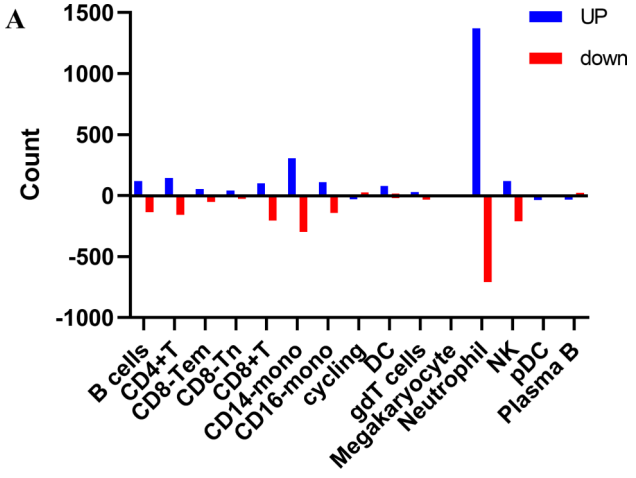

Fig. 4 Overview of DEGs in different cell types. (**A**) Numbers of DEGs across all cell types between the R-irAE and ctrl groups

from extracellular proteins to T cells [29]. Enrichment analysis revealed that the DEGs of CD4-CTL cells were enriched mainly in antigen processing and presentation, cell adhesion molecules, Th17 cell differentiation, phagosome, Th1 and Th2 cell differentiation, and natural killer cell-mediated cytotoxicity signalling pathways (Fig. 8B). These DEGs are involved in the biological processes of cytoplasmic translation, immune system processes, and cell death.

FOS, RPS26, and *JUN* were the top three upregulated genes in CD4-Tn cells, and the most downregulated gene was ITM2A (Fig. 9A). ITM2A, which encodes a type II membrane protein, is reportedly downregulated in breast cancer and can inhibit the cell growth and reduce the aggressiveness of breast cancer [30]. Enrichment analysis revealed that the DEGs of the CD4-Tn cells were enriched mainly in the apoptosis pathway and in the TNF, IL-17, MAPK, T-cell receptor, NF-kappa B, and ferroptosis signalling pathways (Fig. 9B). These DEGs are involved in the biological processes of cytoplasmic translation, immune system development, cell death, and the regulation of protein matabolism (Fig. 9C).

RPS26, *JUN*, and *FOS* were the top three upregulated genes in LIMS1-CD4T cells (Fig. 10A). The enrichment analysis suggested that the DEGs of LIMS1-CD4T cells were enriched in the IL-17, TNF, and Th17 cell differentiation pathways and the Th1 and Th2 cell differentiation signalling pathways (Fig. 10B). These DEGs are involved in the biological processes of cytoplasmic translation and immune system development (Fig. 10C).

FOS, *JUN*, and *DUSP1* were the top three upregulated genes in Th2 cells (Fig. 11A). *DUSP1* is a negative feedback regulator of mitogen-activated protein kinase

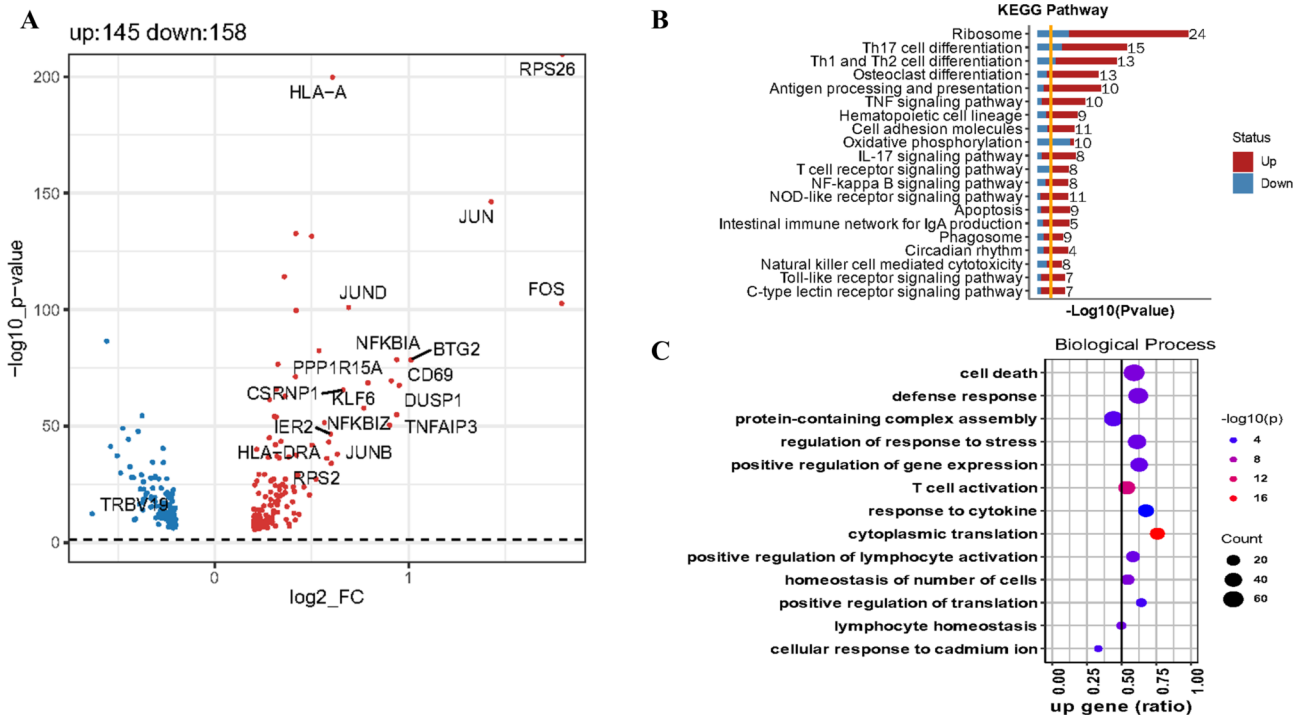

Fig. 5 DEGs and their functions in CD4$^+$T cells. (**A**) The DEGs in CD4$^+$ T cells between the R-irAE and ctrl groups. (**B**) KEGG analysis of the DEGs. (**C**) Enriched biological processes of the DEGs

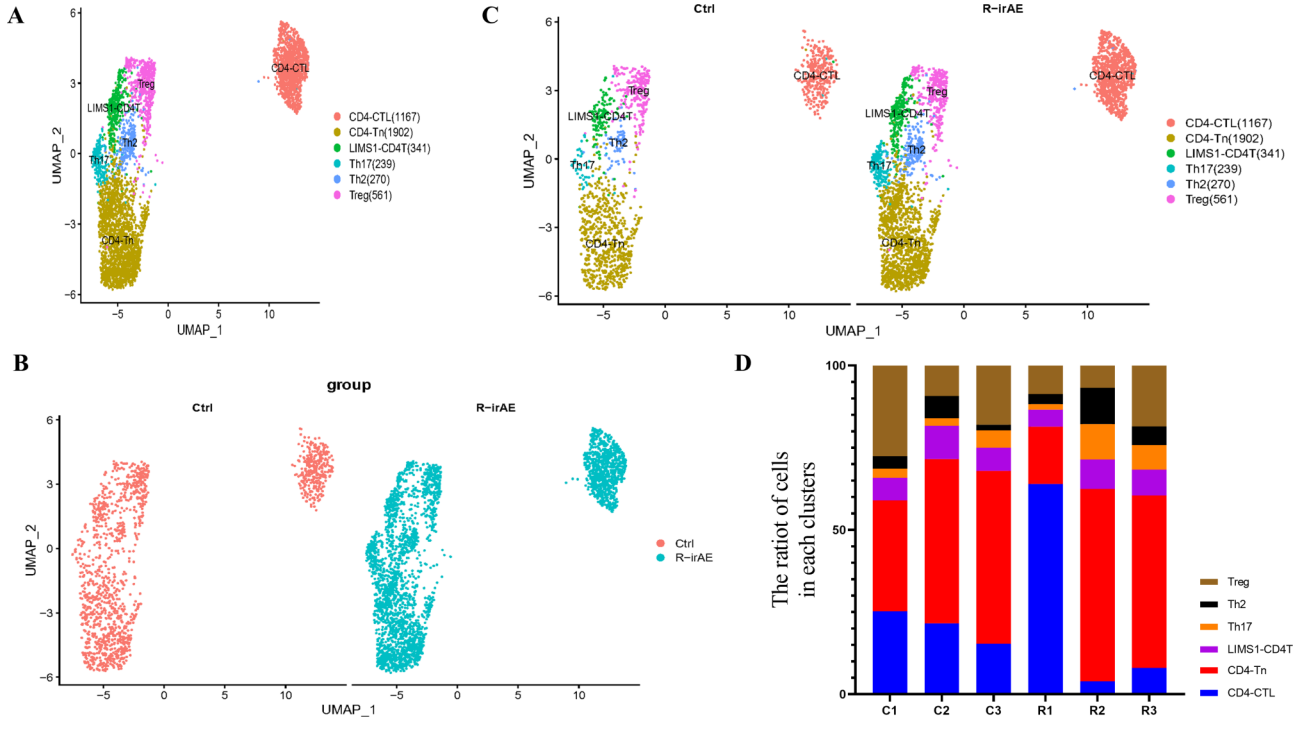

Fig. 6 Immunological features of CD4$^+$T cell subsets. (**A**) UMAP projection of CD4$^+$ T cells. (**B**) UMAP projection of the ctrl and R-irAE conditions. (**C**) The UMAP plot showing CD4$^+$ T cell subsets from the ctrl and R-irAE groups. (**D**) Stacked bar graphs showing the cell type distributions in each sample. The plot is coloured according to the cell type, and each dot corresponds to a single cell

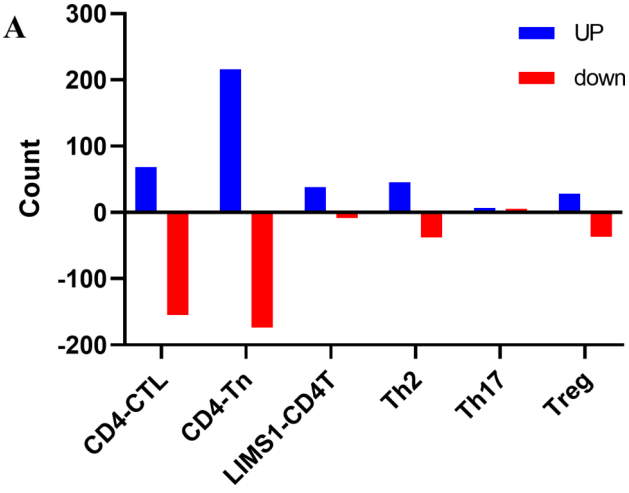

Fig. 7 Overview of DEGs in CD4$^+$T subsets. (**A**) Numbers of subsets of CD4$^+$ T cells in DEGs between the R-irAE and ctrl groups

(MAPK) signalling pathways, which could be important in Th1/Th2 polarization [31]. The enrichment analysis suggested that the DEGs of Th2 cells were enriched in pathways related to cell adhesion molecules, oxytocin, mitophagy, antigen processing and presentation (Fig. 11B). These DEGs are involved in the biological processes of cytoplasmic translation and rRNA processing (Fig. 11C).

FOS, *RPS26*, and *JUN* were the top three upregulated genes in Th17 cells (Figure S2). Given that there were only a small number of DEGs in Treg cells, enrichment analyses could not be performed.

FOS, *RPS26*, and *JUND* were the top three upregulated genes in Treg cells (Fig. 12A). *JUND* is a member of the JUN family. This protein has been proposed to protect cells from p53-dependent senescence and apoptosis [32].

Characteristics and biological functions of CD8+ T cells

There are three cell types of CD8$^+$ T cells: CD8-Tem, CD8$^+$ T, and CD8-Tn cells. Considering that CD8-Tem and CD8-Tn cells were present in extremely small numbers, we focused on CD8$^+$ T cells. *RPS26*, *TRBV25-1*, and *JUN* were the top three upregulated genes in CD8$^+$ T cells (Fig. 13A). *TRBV25-1* belongs to the T-cell receptor (TCR) beta chain variable gene (TRBV) family. The *TRBV*, *TRBD*, and *TRBJ* genes encode regions of CDR3β in the beta chains of the TCR, which is responsible for interactions with antigenic peptides.

The DEGs of the CD8$^+$ T cells were enriched in Th17 cell differentiation, Th1 and Th2 cell differentiation, antigen processing and presentation, the intestinal immune network for IgA production, NK cell-mediated cytotoxicity, the T-cell receptor signalling pathway, the phagosome, and cell adhesion molecules (Fig. 13B).

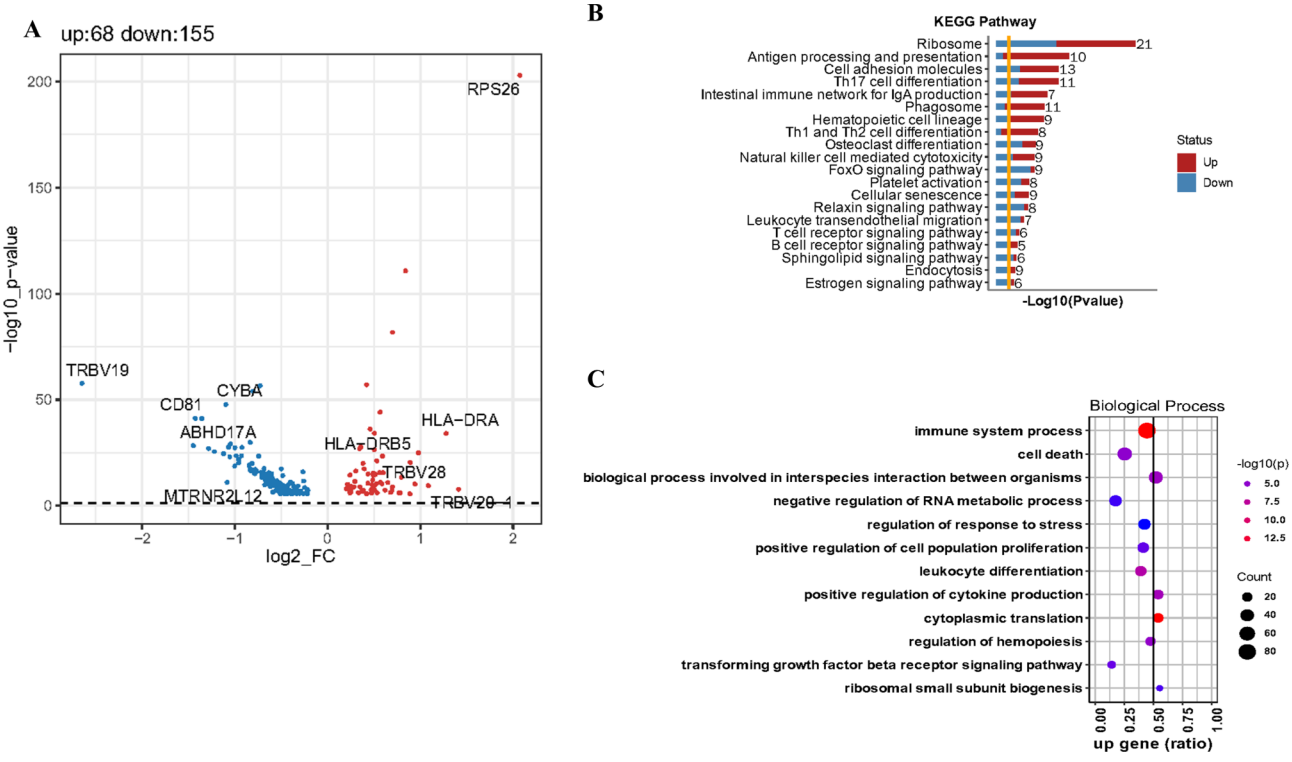

Fig. 8 DEGs and their functions in CD4-CTL cells. (**A**) The DEGs of CD4-CTL cells between the R-irAE and ctrl groups. (**B**) KEGG pathway analysis of the DEGs. (**C**) Dot plot of the enriched biological processes of the DEGs

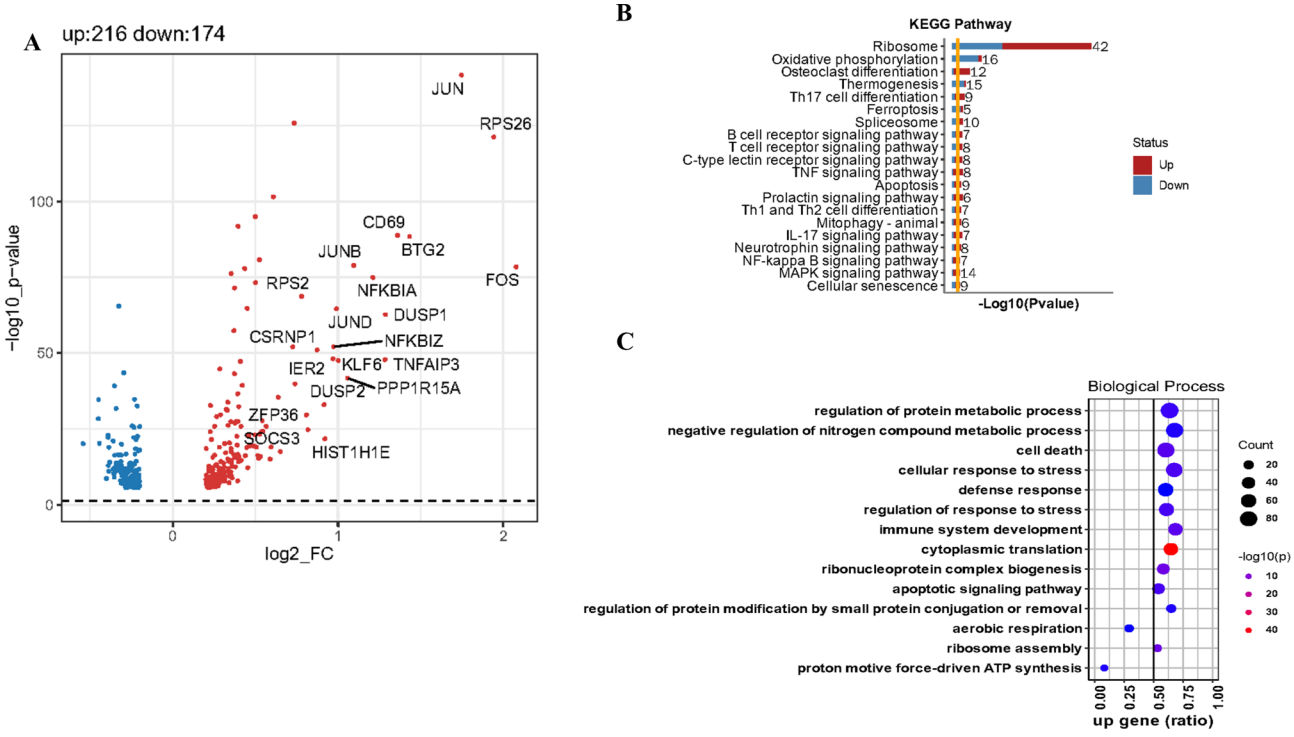

Fig. 9 DEGs and their functions in CD4-Tn cells. (**A**) The DEGs of CD4-Tn cells between the R-irAE and ctrl groups. (**B**) KEGG pathway analysis of the DEGs. (**C**) Dot plot of the enriched biological processes of the DEGs

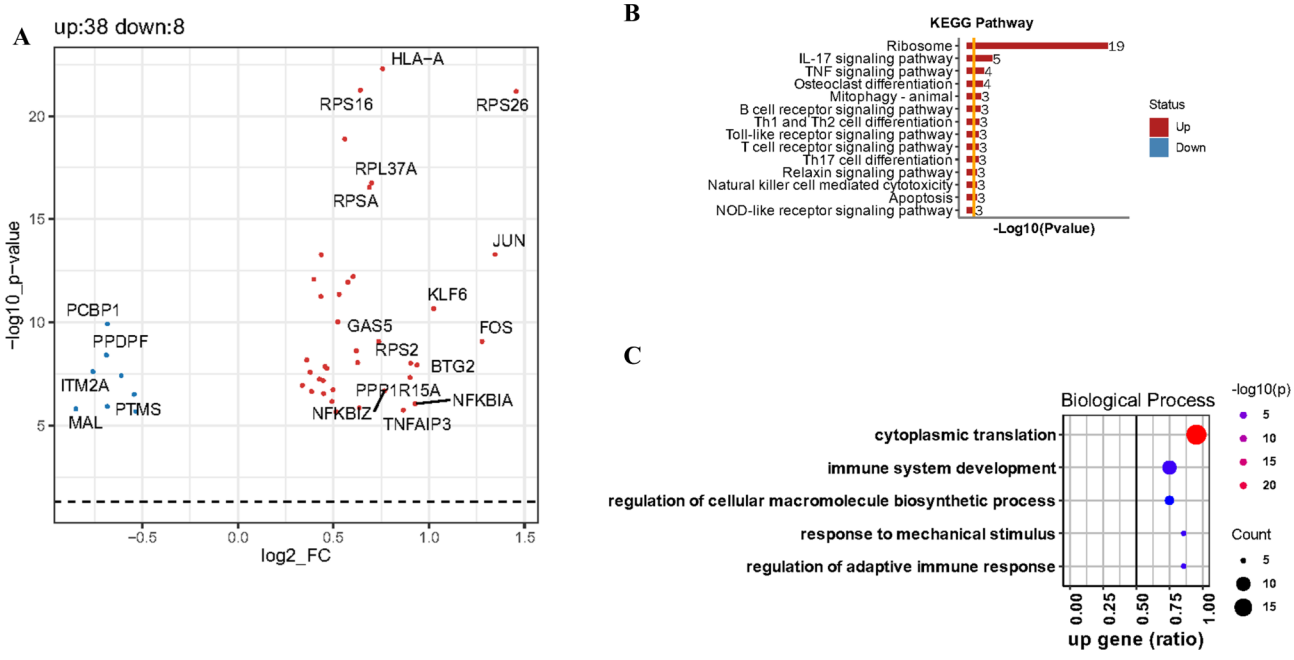

Fig. 10 DEGs and their functions in LIMS1-CD4T cells. (**A**) The DEGs in LIMS1-CD4T cells between the R-irAE and ctrl groups. (**B**) KEGG pathway analysis of the DEGs. (**C**) Dot plot of the enriched biological processes of the DEGs

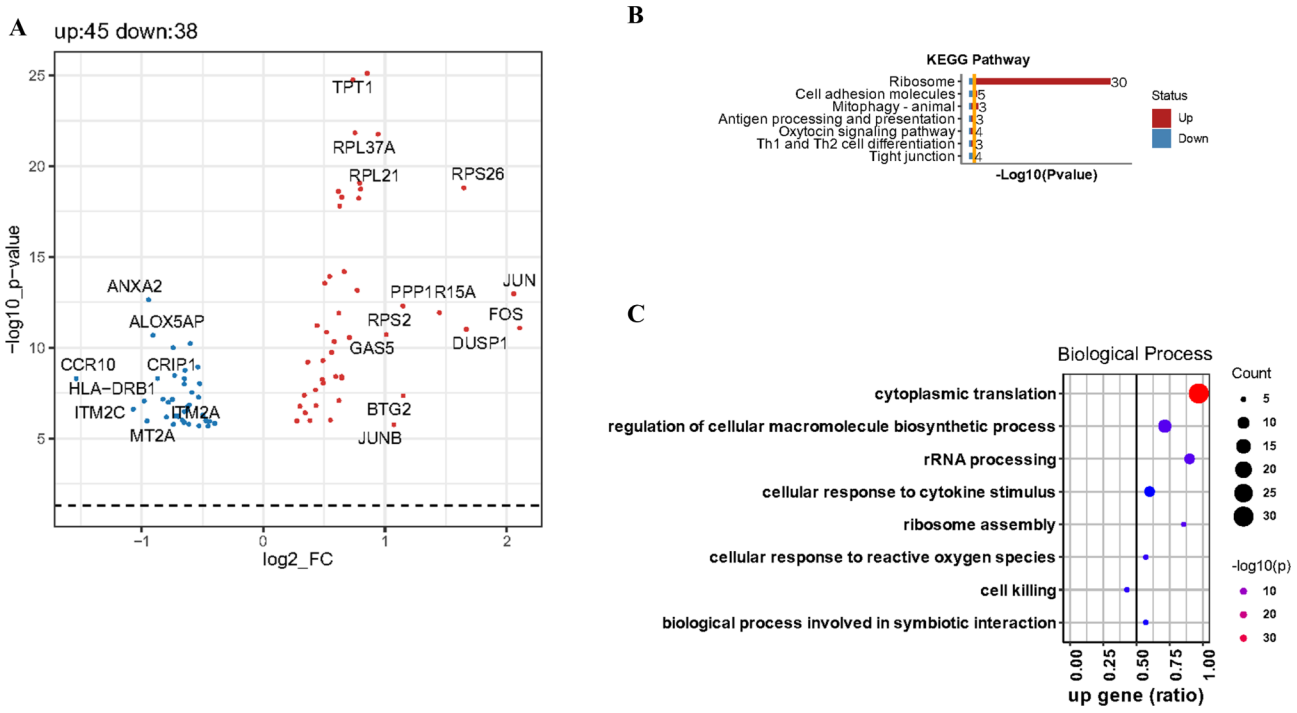

Fig. 11 DEGs and their functions in Th2 cells. (**A**) The DEGs in Th2 cells between the R-irAE and ctrl groups. (**B**) KEGG pathway analysis of the DEGs. (**C**) Dot plot of the enriched biological processes of the DEGs

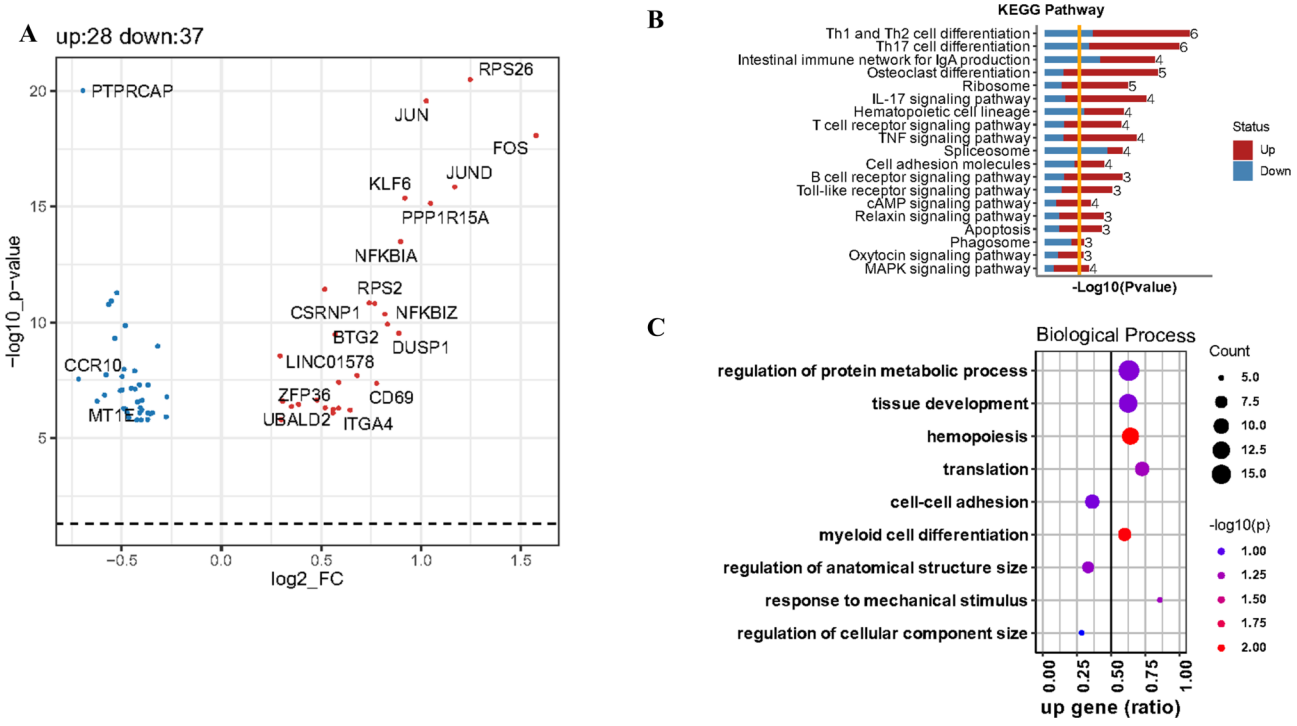

Fig. 12 DEGs and their functions in Treg cells. (**A**) The DEGs in Th2 cells between the R-irAE and ctrl groups. (**B**) KEGG pathway analysis of the DEGs. (**C**) Dot plot of the enriched biological processes of the DEGs

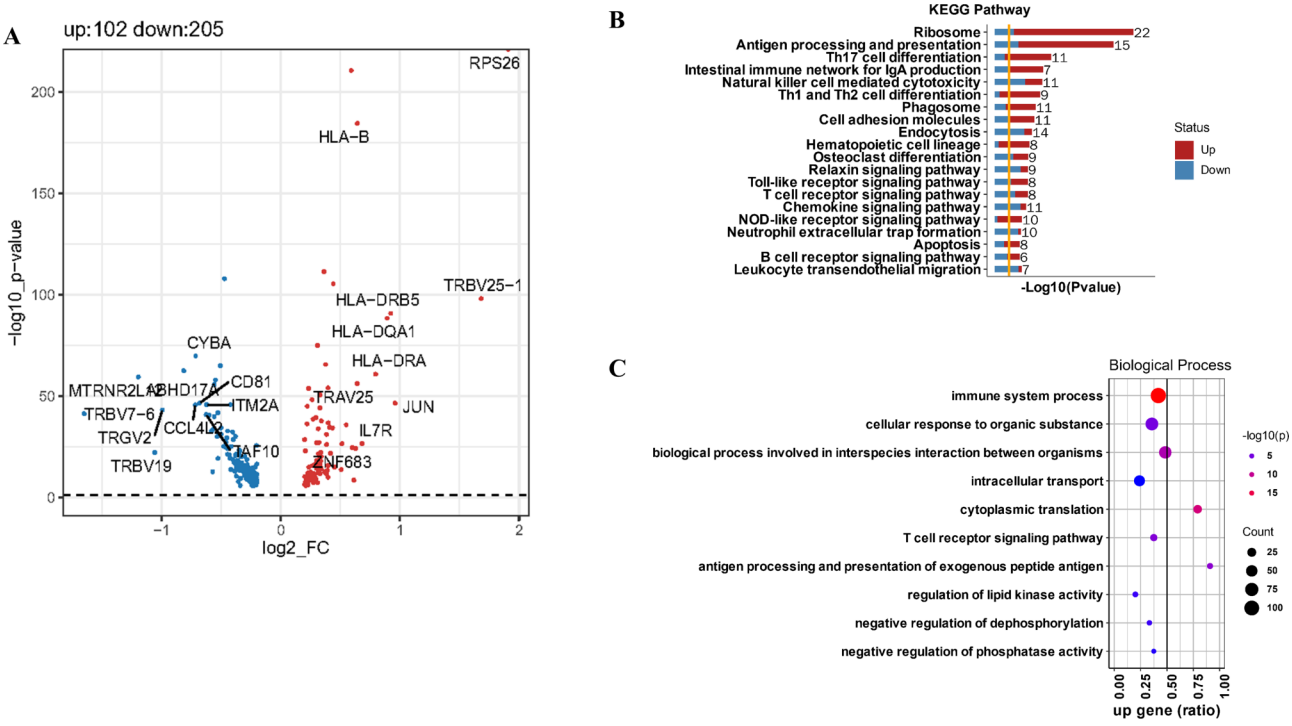

Fig. 13 DEGs and their functions in CD8$^+$T cells. (**A**) The DEGs of CD8$^+$ T cells between the R-irAE and ctrl groups. (**B**) KEGG pathway analysis of the DEGs. (**C**) Dot plot of the enriched biological processes of the DEGs

These DEGs were found to be responsible for the biological processes of cytoplasmic translation, antigen processing and presentation of exogenous peptide antigens, regulation of lipid kinase activity, and the T-cell receptor signaling pathway (Fig. 13C).

Discussion

In recent years, the advent of ICIs has revolutionized the field of oncology. However, the ICI-related renal toxicity has attracted the attention of oncologists and nephrologists. The occurrence of ICI-related AKI may warrant the interruption of tumour treatment. Consequently, studies on the mechanisms of ICI-related AKI are urgently needed.

Although the mechanisms underlying PD-1-associated renal toxicity have not been elucidated, some hypotheses have been proposed through some clinical studies and mouse experiments; these hypothesis include loss of tolerance versus self-antigens, reactivation of drug-specific T cells, proinflammatory cytokines, and off-target effects [33]. On the basis of these studies, we focused on CD8$^+$ T cells and CD4$^+$ T cells. In this research, we applied scRNA-seq technology to reveal the features of PBMCs from lung cancer patients who developed R-irAEs due to PD-1 therapy. Fifteen clusters were identified. We were concerned about the DEGs, the pathways in which they were enriched, and the biological functions of CD4$^+$ T and CD8$^+$ T cells as we noted no significant differences in the proportion of each cluster between the R-irAE and ctrl groups. RPS26 and JUN were both the top upregulated genes in both CD4$^+$ T cells and CD8$^+$ T cells. The DEGs of CD4 + T cells and CD8 + T cells were enriched in Th17, Th1, and Th2 cell differentiation, and NK cell-mediated cytotoxicity signalling pathways. These results suggest that we may focus on these genes and pathways in future studies and that these genes and pathways may be targets for the treatment of PD-1-induced AKI.

Despite some notable results, this study has some limitations. First, the sample size was small, and studies with larger sample sizes are needed in the future. Only male patients were included, and the inclusion of female patients needs to be considered in the future. Second, no kidney specimens were obtained in this study because of the poor physical fitness of the patients and the lack of patient consent to undergo renal biopsy. Therefore, for subsequent research, we collected PBMCs from lung cancer patients treated with PD-1 inhibitors. We used PBMC samples for scRNA-seq, but these samples do not directly reflect the changes in the immune profile associated with PD-1 related AKI. Since there were no renal specimens, PD-1 induced AKI was not confirmed by renal biopsy in this study. The diagnosis of PD-1-induced AKI is empirical. On the basis of abnormal sCr,

potential nephrotoxic drugs and other causes of renal impairment such as dehydration, infection, and urinary tract obstruction were excluded. Many studies have reported that increased sCr level occurring alongside proteinuria, haematuria, and pyuria are symptoms of AKI caused by ICI treatment. In our study, all three patients with R-irAEs had elevated sCr levels. These findings indicate that patients should be closely monitored for changes in sCr levels in the urine. Finally, we did not analyse intercellular communication, which may have revealed some potential mechanisms.

Taken together, this study explored the immune mechanisms of PD-1-related R-irAEs in patients with lung cancer via scRNA-seq. The DEGs and enriched pathways may be novel markers of R-irAEs caused by anti-PD-1 therapy.

Abbreviations

ICIs	Immune checkpoint inhibitors
irAEs	Immune-related adverse events
PD-1	Programmed cell death protein 1
R- irAEs	S- Renal irAEs
PBMCs	Peripheral blood mononuclear cells
DEGs	Differentially expressed genes
KEGG	Kyoto Encyclopedia of Genes and Genomes
GO	Gene ontology
CTLA-4	Cytotoxic T-lymphocyte-associated protein 4
PD-L1	Programmed death-ligand 1
FDA	Food and Drug Administration
Treg	regulatory T
NK	Natural killer
Scr	Serum creatinine
AKI	Acute kidney injury
AIN	Acute interstitial nephritis
MCD	Minimal change disease
MN	Membranous nephropathy
scRNA-seq	Single-cell RNA sequencing
EDTA	Ethylenediaminetetraacetic acid
UMI	Unique molecular identifier
UMAP	Uniform manifold approximation and projection
CTL-CD4	Cytotoxic $CD4^+$ T cells
CD8-Tem	$CD8^+$ T effector memory
CD8-Tn	Naïve $CD8^+$ T
DCs	Dendritic cells
pDCs	Plasmacytoid dendritic cells
MAPK	Mitogen-activated protein kinase
TCR	T-cell receptor
TRBC	T-cell receptor beta chain variable gene

Supplementary Information

The online version contains supplementary material available at https://doi.org/10.1186/s12882-024-03754-0.

Supplementary Material 1

Acknowledgements
The authors thank the patients for their contributions to this research.

Author contributions
ShuSu Liu performed single cell analysis and wrote the manuscript. PeiYu Lu collected the samples and wrote the manuscript. BiXia Yang collected the samples. Yan Yang performed the data analysis of scRNA-seq. Hua Zhou and Min Yang were responsible for the study concept, design, and revision. All authors reviewed the manuscript.

Funding
This work was supported by Top Talent of Changzhou "The 14th Five-year Plan" High-Level Health Talents Training Project (No. 2022260), the Changzhou Key Medical Discipline (No. CZXK202204), the Changzhou Science and Technology Program (No. CJ20220222), and the Young Talent Development Plan of Changzhou Health Commission (No. CZQM2023002).

Data availability
All data presented in this research are accessible through the GEO series accession number GSE242780 (https://www.ncbi.nlm.nih.gov/geo/query/acc.cgi?acc=GSE242780).

Declarations

Ethical approval
The study was approved by the ethics committee of the Third Affiliated Hospital of Soochow University (Grant No. 2022[039]). The study protocol adhered to the Declaration of Helsinki.

Consent for publication
Not applicable.

Informed consent
All patients signed an informed consent before enrolment in the study.

Competing interests
The authors declare no competing interests.

Author details
[1]Department of Nephrology, The Third Affiliated Hospital of Soochow University, Changzhou 213003, China

Received: 14 November 2023 / Accepted: 11 September 2024
Published online: 14 September 2024

References

1. Darnell Eli P, Mooradian Meghan J, Baruch Erez N, et al. Immune-related adverse events (irAEs): diagnosis, management, and clinical Pearls[J]. Curr Oncol Rep. 2020;22(4):39.
2. Chennamadhavuni Adithya A, Laith J, Ning, et al. Risk factors and biomarkers for Immune-related adverse events: a practical guide to identifying high-risk patients and rechallenging Immune Checkpoint Inhibitors[J]. Front Immunol. 2022;13:779691.
3. Das Satya J, Douglas B. Immune-related adverse events and anti-tumor efficacy of immune checkpoint inhibitors[J]. J Immunother Cancer. 2019;7(1):306.
4. Pardoll Drew M. The blockade of immune checkpoints in cancer immunotherapy[J]. Nat Rev Cancer. 2012;12(4):252–64.
5. Tocheva Anna S, Mor A. Checkpoint inhibitors: applications for Autoimmunity[J]. Curr Allergy Asthma Rep. 2017;17(10):72.
6. Okazaki Taku C, Shunsuke I, Yoshiko, et al. A rheostat for immune responses: the unique properties of PD-1 and their advantages for clinical application[J]. Nat Immunol. 2013;14(12):1212–8.
7. Wang Daniel Y, Salem Joe-Elie C, Justine V, et al. Fatal toxic effects Associated with Immune Checkpoint inhibitors: a systematic review and Meta-analysis[J]. JAMA Oncol. 2018;4(12):1721–8.
8. Lee DJ, Lee Howard J, Farmer Jocelyn R, et al. Mechanisms driving Immune-related adverse events in Cancer patients treated with Immune Checkpoint Inhibitors[J]. Curr Cardiol Rep. 2021;23(8):98.
9. Yamaguchi Atsushi S, Yoshitaka N, Katsuya, et al. Association between skin immune-related adverse events (irAEs) and multisystem irAEs during PD-1/PD-L1 inhibitor monotherapy[J]. J Cancer Res Clin Oncol. 2022;149(4):1659–66.
10. Yamada Kentaro S, Tsunaki N, Masanao, et al. Clinical characteristics of gastrointestinal immune-related adverse events of immune checkpoint inhibitors and their association with survival[J]. World J Gastroenterol. 2021;27(41):7190–206.
11. Naidoo Jarushka C, Tricia R, Lipson Evan J et al. Chronic immune checkpoint inhibitor pneumonitis[J]. J Immunother Cancer, 2020, 8(1).

12. Thoetchai P, Jennifer W, Matthew O. Hepatotoxicity from Immune Checkpoint inhibitors: a systematic review and management Recommendation[J]. Hepatology. 2020;72(1):315–29.
13. Iwama Shintaro K, Tomoko AH. Clinical characteristics, management, and potential biomarkers of Endocrine Dysfunction Induced by Immune Checkpoint Inhibitors[J]. Endocrinol Metabolism. 2021;36(2):312–21.
14. Rafeh NA, Moey Melissa Y, Natash CT, Xiao-Wei, et al. Major adverse cardiac events with Immune Checkpoint inhibitors: a pooled analysis of trials Sponsored by the National Cancer Institute-Cancer therapy evaluation Program[J]. J Clin Oncol. 2022;40(29):3439–52.
15. Isik Busra, Alexander Mariam P, Manohar Sandhya, et al. Biomarkers, clinical features, and rechallenge for Immune checkpoint inhibitor Renal Immune-related adverse Events[J]. Kidney Int Rep. 2021;6(4):1022–31.
16. Smithy James W, Faleck David PMA. Facts and hopes in prediction, diagnosis, and treatment of Immune-related adverse Events[J]. Clin Cancer Res. 2022;28(7):1250–7.
17. Khoja L, Day D, Wei-Wu Chen T, et al. Tumour- and class-specific patterns of immune-related adverse events of immune checkpoint inhibitors: a systematic review [J]. Ann Oncol. 2017;28(10):2377–85.
18. Wanchoo Rimda K, Sabine U, Nupur N, et al. Adverse renal effects of Immune Checkpoint inhibitors: a narrative Review[J]. Am J Nephrol. 2017;45(2):160–9.
19. Sorah Jonathan D, Rose Tracy L, Radhakrishna Roshni, et al. Incidence and prediction of Immune Checkpoint inhibitor-related Nephrotoxicity[J]. J Immunother. 2021;44(3):127–31.
20. Seethapathy Harish Z, Sophia, Chute Donald F, et al. The incidence, causes, and risk factors of Acute kidney Injury in patients receiving Immune Checkpoint Inhibitors[J]. Clin J Am Soc Nephrol. 2019;14(12):1692–700.
21. Longhitano Elisa M, Paola LR, Claudia et al. Immune Checkpoint inhibitors and the kidney: a focus on diagnosis and management for Personalised Medicine[J]. Cancers, 2023, 15(6).
22. Rongrong H, Xu CM. Renal immune-related adverse events of immune checkpoint inhibitor[J]. Asia-Pac J Clin Oncol. 2020;16(6):305–11.
23. Murakami Naoka M, Shveta, Riella Leonardo V. Renal complications of immune checkpoint blockade[J]. Curr Probl Cancer. 2016;41(2):100–10.
24. Domínguez C, Cecilia X, Chuan J, Lorna B, et al. Cross-tissue immune cell analysis reveals tissue-specific features in humans[J]. Science. 2022;376(6594):eabl5197.
25. Murakami Naoka, Borges Thiago J, Yamashita Michifumi, et al. Severe acute interstitial nephritis after combination immune-checkpoint inhibitor therapy for metastatic melanoma[J]. Clin Kidney J. 2016;9(3):411–7.
26. Cortazar Frank B, Marrone Kristen A, Troxell Megan L, et al. Clinicopathological features of acute kidney injury associated with immune checkpoint inhibitors[J]. Kidney Int. 2016;90(3):638–47.
27. Shivtia T-S, Yehudith A, Reuven O. Early cell-cycle gene expression in T-cells after hematopoietic stem cell transplantation[J]. Transpl Immunol. 2013;29(1–4):146–54.
28. Chen Zhejun Z, Kaiqiong TM, et al. A single-cell survey of the human glomerulonephritis[J]. J Cell Mol Med. 2021;25(10):4684–95.
29. International MHC, Network AG, John R, Goyette D, Philippe, et al. Mapping of multiple susceptibility variants within the MHC region for 7 immune-mediated diseases[J]. PNAS. 2009;106(44):18680–5.
30. Zhang Rui X, Tao X, Yu, et al. ITM2A as a tumor suppressor and its correlation with PD-L1 in breast Cancer[J]. Front Oncol. 2021;10:581733.
31. Kirk Sean G, Samavati Lobelia L, Yusen. MAP kinase phosphatase-1, a gatekeeper of the acute innate immune response[J]. Life Sci. 2019;241:117157.
32. Paneni F, Osto E, Costantino S, et al. Deletion of the activated protein-1 transcription factor JunD induces oxidative stress and accelerates age-related endothelial dysfunction[J]. Circulation. 2013;127(11):1229–e21.
33. Franzin Rossana NG, Stefano S, Federica, et al. The Use of Immune checkpoint inhibitors in Oncology and the occurrence of AKI: where do we Stand[J]. Front Immunol. 2020;11:574271.

Publisher's note